Left inferior parietal lobe engagement in social cognition and language

Danilo Bzdok[1,2,3,4,5,*,#], **Gesa Hartwigsen**[6,#], **Andrew Reid**[3], **Angela R. Laird**[7], **Peter T. Fox**[8], and **Simon B. Eickhoff**[3,4]

[1]Department of Psychiatry, Psychotherapy and Psychosomatics, RWTH Aachen University, Germany

[2]JARA, Translational Brain Medicine, Aachen

[3]Institute of Neuroscience and Medicine (INM-1), Research Center Jülich, Jülich, Germany

[4]Institute of Clinical Neuroscience and Medical Psychology, Heinrich Heine University, Düsseldorf, Germany

[5]Parietal team, INRIA, Neurospin, bat 145, CEA Saclay, 91191 Gif-sur-Yvette, France

[6]Department of Psychology, Christian-Albrechts-University Kiel, Kiel, Germany

[7]Department of Physics, Florida International University, USA

[8]Research Imaging Institute, University of Texas Health Science Center, San Antonio, TX, USA

Abstract

Social cognition and language are two core features of the human species. Despite distributed recruitment of brain regions in each mental capacity, the left parietal lobe (LPL) represents a zone of topographical convergence. The present study quantitatively summarizes hundreds of neuroimaging studies on social cognition and language. Using connectivity-based parcellation on a meta-analytically defined volume of interest (VOI), regional coactivation patterns within this VOI allowed identifying distinct subregions. Across parcellation solutions, two clusters emerged consistently in rostro-ventral and caudo-ventral aspects of the parietal VOI. Both clusters were functionally significantly associated with social-cognitive and language processing. In particular, the rostro-ventral cluster was associated with lower-level processing facets, while the caudo-ventral cluster was associated with higher-level processing facets in both mental capacities. Contrarily, in the (less stable) dorsal parietal VOI, all clusters reflected computation of general-purpose processes, such as working memory and matching tasks, that are frequently co-recruited by social or language processes. Our results hence favour a rostro-caudal distinction of lower-

*Correspondence should be addressed to: Prof. Dr. Dr. Danilo Bzdok, Klinik für Psychiatrie, Psychotherapie und Psychosomatik, Pauwelsstraße 30, 52074 Aachen, Germany, Phone: +49 241 8085729, danilo.bzdok@rwth-aachen.de.
#These authors contributed equally to this work

versus higher-level processes underlying social cognition and language in the left inferior parietal lobe.

Keywords

theory of mind; speech; statistical learning; connectivity-based parcellation; functional connectivity; functional decoding

1. Introduction

Human cognitive evolution has been leveraged by social and language capacities. A prominent feature of social cognition is the ability to infer the thoughts, beliefs and behavioral dispositions of other people. Even young infants at the age of seven months appear capable of implicit mental inference (Frith and Frith, 2003). In particular, they successfully ascribe false beliefs to agents, reflecting a likely understanding that an agent can have incorrect beliefs about the physical world (Kovacs et al., 2010). This provides evidence for an early development of advanced social-cognitive functions (Kovacs et al., 2010; Onishi and Baillargeon, 2005; Surian et al., 2007). Successful perspective-taking is essential for navigation of the inter-personal space. It enables us to collaborate with our peers (Engemann et al., 2012; Watson et al., 1999), thus promoting the social relations that form the basis of both local communities and global society (Tomasello et al., 2005).

Social cognition is closely intertwined with language comprehension and production. Both processes appear crucial for inter-personal exchange. From an evolutionary perspective, the use of language might facilitate successful bonding of (larger) social groups. In particular, language might have evolved to facilitate the exchange of social information (Dunbar, 2004). Indeed, previous studies have suggested that social topics account for approximately two thirds of human communication across age and gender (Dunbar et al., 1997).

Language is an elementary mental faculty that serves inter-individual communication. A key facet of language processing is the association of sounds and symbols with meaningful concepts (i.e., semantic processing), which enables us to describe our external environment and articulate abstract thought (Price, 2000). The understanding of the semantic implications of a given context is of particular relevance for social interactions. It was argued that semantic processing is mandatory for our ability to act in a coherent, purposeful manner regarding the meaning of words, objects, or situations (Lambon Ralph and Patterson, 2008). Moreover, semantic processing plays a particular role in a diverse set of higher-level cognitive processes, contributing to both social cognition and language. These cognitive facets include sentence comprehension, discourse, problem solving, and planning (Binder and Desai, 2011; Binder et al., 2009). Taking these psychological categories to the neurobiological level, mental representations related to others' thoughts and to language content might feature a shared representation as common denominator: the expression of propositional or sentence-like, logical content (Cohen et al., 2014).

In sum, the above-cited studies suggest a strong functional interaction between social cognition and language. However, it remains unclear whether this interaction might also be

underpinned by a shared functional-anatomical network. Indeed, the neural correlates common to social cognition and language are currently under-researched. Informal juxtaposition of previous neuroimaging reports on social cognition and language strongly suggests common involvement of heteromodal association areas. High-level social cognition tasks, on the one hand, typically modulate neural activity in the medial prefrontal cortex, posterior cingulate cortex / precuneus and bilateral temporo-parietal junction of the parietal lobe (Mar, 2011). Language tasks, on the other hand, typically engage the inferior frontal gyrus, posterior superior temporal gyrus as well as the angular gyrus and supramarginal gyrus of the left parietal lobe. Hence, it might be the left parietal lobe (LPL) that is commonly recruited in social cognition and language tasks (Binder et al., 2009). Indeed, previous neuroimaging and virtual lesion studies with non-invasive brain stimulation have demonstrated a key contribution of different LPL subregions to a variety of different social cognitive capacities (Bzdok et al., 2013b; Decety and Lamm, 2007; Spreng et al., 2009) and language capacities (e.g., Binder et al., 2009; Hartwigsen et al., 2014).

The inferior parietal lobe, in particular, might have expanded in the primate lineage (Orban et al., 2004), while existence of its nonhuman homologue is currently uncertain (Mars et al., 2011; Seghier, 2013). Such expansion might relate to our unique capacity of speech and language processing and the ability for planning, problem solving and other complex processes (Binder and Desai, 2011). More specifically, an LPL subregion extending into the superior temporal gyrus turned out to be a key player of converging semantic information pathways (Binder et al., 2009). In studies of social cognition, this region is frequently labeled as "temporo-parietal junction" and "posterior superior temporal sulcus". In contrast, the language literature often refers to the same region as "angular gyrus" and "posterior superior temporal gyrus / sulcus". *For the sake of simplicity, these mostly parietal regions, extending into adjacent temporal regions, will henceforth be referred to as "LPL".* We opted for this functionally, rather than strictly neuroanatomically, motivated term because neural activity associated with the two target cognitive processes routinely exceeds traditional macroscopical landmarks.

Taken together, previous evidence converges to a functional contribution of the LPL to social cognition and language. However, it is unclear whether both functions engage the same anatomical regions of the LPL. *It is therefore open to debate whether different subregions in the LPL contribute to different processing facets underlying social cognition and language. This question is addressed by the present study.* First, we conducted connectivity-based parcellation of a volume of interest (VOI) in the LPL (Eickhoff et al., 2011; Johansen-Berg et al., 2004). Second, the ensuing connectivity-derived subregions in the LPL were characterized by determining their brain-wide connectivity profiles based on task-related meta-analytic connectivity-modeling (MACM) and task-unrelated resting-state correlations (RSFC). Finally, we inferred the functional associations of the derived subregions from extensive meta-data in the BrainMap archive (Fox and Lancaster, 2002). In this way, the present report provides a statistically defensible characterization of subdivisions, connectivity, and functions of the human left parietal lobe in social and language processes.

2. Materials and methods

In this section, we first provide a step-by-step overview of our study and then describe each of these steps in detail.

2.1. Workflow

As a prerequisite for meta-analytic connectivity mapping, we first defined the volume of interest (section 2.2.). This was achieved by computing converging activation in the left lateral parietal cortex across social cognitive and language tasks. In a second step, we computed an activation likelihood estimation (ALE) meta-analysis to quantitatively map the whole-brain coactivation profile of each voxel within the obtained VOI in the lateral parietal cortex (section 2.3.). The seed voxels were then grouped by k-means clustering (Eickhoff et al., 2015) based on similarities of their coactivation profiles (i.e., connectivity based parcellation, section 2.4.). In the next step, the optimal filter range was selected as a prerequisite for determining the optimal cluster solution (section 2.5.) The most pertinent clustering solution was then identified by the combination of different metrics (section 2.6.). The whole-brain connectivity patterns of each derived cluster (i.e., subregion within the LPL VOI) was determined based on meta-analytic connectivity modeling (Eickhoff et al., 2011; Robinson et al., 2010) (section 2.7.) and resting-state functional connectivity (Biswal et al., 1995; Yeo et al., 2011) (section 2.8.). The final step of our analyses included the characterization of the clusters based on an overlap between task-dependent and task-independent connectivity (section 2.9) and the characterization of cluster function (functional decoding, section 2.10.). Anatomical localization was performed by means of the SPM Anatomy Toolbox (Eickhoff et al., 2007; Eickhoff et al., 2005) (section 2.11.).

2.2. Defining the volume of interest in the left lateral parietal lobe

This study aims to functionally segregate the left lateral parietal lobe in social and language tasks. Convergence of parietal activation across both task families was determined by coordinate-based meta-analysis (Eickhoff et al., 2012; Turkeltaub et al., 2002). High-level social processing was represented by a previous meta-analysis on 68 theory of mind experiments (Bzdok et al., 2012). General language processing was localized by a present meta-analysis on all language-associated taxonomy terms (i.e., orthography, speech, syntax, semantics, and phonology) from the BrainMap database (Fox and Lancaster, 2002), which amounted to 1841 experiments. The converged activation (i.e., OR-conjunction) in the lateral parietal cortex was then extracted from each meta-analysis and merged into a composite region (Figure 1). Please appreciate that the location of the LPL VOI was thus determined in a *functional* rather than anatomical fashion. That is, *notions of cognitive theory, not micro- or macro-anatomical landmarks, constrained the starting point of the present investigation*. The meta-analytic composite convergence was subject to spatial smoothing by iterative voxel-wise image dilation (i.e., adding an outer voxel layer) and erosion (i.e., removing an outer voxel layer). The ensuing more regular meta-analytic convergence definition constituted the VOI for all subsequent analyses.

2.3. Meta-analytic connectivity modeling

Computation of whole-brain coactivation maps for each voxel of the VOI was performed based on the BrainMap database (www.brainmap.org; Fox and Lancaster, 2002; Laird et al., 2011). We limited our analysis to functional neuroimaging studies in the healthy human brain (no interventions, no group comparisons), which reported results as coordinates in stereotaxic standard space. These inclusion criteria yielded ~7,500 eligible experiments at the time of analysis (September 2014). Please note that we considered all eligible BrainMap experiments because any pre-selection based on taxonomic categories would have constituted a strong a priori hypothesis about how brain networks are organized. However, it remains elusive how well psychological constructs, such as emotion and cognition, map on regional brain responses (Laird et al., 2009; Mesulam, 1998; Poldrack, 2006).

The rationale of coactivation analysis is to compute the convergence across (all foci of) those BrainMap experiments where the seed voxel in question is reported as active (Laird et al., 2013). One challenge in constructing voxel-wise coactivation maps is the limited number of experiments activating precisely at any particular seed voxel. Hence, pooling across the close spatial neighborhood has become the dominant approach in MACM analysis (Eickhoff et al., 2011) to enable a reliable characterization of task-based functional connectivity. Importantly, the extent of this spatial filter was systematically varied from including the closest 20 to 200 experiments in steps of two (Clos et al., 2013). That is, we selected the sets of 20, 22, 24, ..., 198, 200 experiments reporting the closest activation at a given seed voxel (i.e., 91 filter sizes). This was implemented by calculating and subsequently sorting the Euclidean distances between a given seed voxel and any activation reported in BrainMap. Then, the x nearest activation foci (i.e., filter size) were associated with that seed voxel.

The retrieved experiments were used to compute the brain-wide coactivation profile of a given seed voxel for each of the 91 filter sizes. In particular, we performed a coordinate-based meta-analysis over all foci reported in these experiments to quantify their convergence. Since the experiments were identified by activation in or near a particular seed voxel, highest convergence was obviously found at the location of the seed. Convergence outside the seed, however, indicated coactivation across task-based functional neuroimaging experiments. These brain-wide coactivation patterns for each individual seed voxel were computed by activation likelihood estimation. The key idea behind ALE is to treat the foci reported in the associated experiments not as single points, but rather as centers for 3D Gaussian probability distributions that reflect the spatial uncertainty associated with neuroimaging results. Using the latest ALE implementation (Eickhoff et al., 2012; Eickhoff et al., 2009; Turkeltaub et al., 2012), the spatial extent of those Gaussian probability distributions was based on empirical estimates of between-subject and between-template variance of neuroimaging foci (Eickhoff et al., 2009). For each experiment, the probability distributions of all reported foci were then combined into a modeled activation (MA) map by the recently introduced "non-additive" approach that prevents local summation effects (Turkeltaub et al., 2012). The voxel-wise union across the MA maps of all experiments associated with the current seed voxel then yielded an ALE score for each voxel of the brain that describes the coactivation probability of that particular location with the current seed

voxel. The ALE scores of all voxels within gray matter (based on 10% probability according to the ICBM maps) were recorded before moving to the next voxel of the seed region.

In sum, quantitative ALE meta-analysis over all foci reported in the experiments associated with the current seed voxel determined how likely any other voxel throughout the brain was to coactivate with that particular seed voxel. Notably, no threshold was applied to the ensuing coactivation maps at this point of analysis to retain the complete pattern of coactivation likelihood (Bzdok et al., 2013b; Cieslik et al., 2013).

2.4. Connectivity-based parcellation by k-means clustering

The unthresholded brain-wide coactivation profiles for all seed voxels were then combined into a N_S x N_T coactivation matrix, where N_S denotes the number of seed voxels (3790 voxels in the present VOI at $2 \times 2 \times 2$ mm³ resolution) and N_T the number of target voxels in the gray matter of the reference brain volume at $4 \times 4 \times 4$ mm³ resolution (~36.000 voxels located within gray matter). Given the use of 91 different filter sizes, this step resulted in 91 individual coactivation matrices, each representing the whole-brain connectivity of the seed voxels at a particular filter size. The parcellation of the VOI was performed using *k*-means clustering (Eickhoff et al., 2015) as implemented in Matlab with $K = 3, 4, 5, 6$ using one minus the correlation between the connectivity patterns of seed voxels as a distance measure (i.e., correlation distance). This parcellation was performed for each of the 91 filter sizes independently, yielding 4 (*k* means cluster solutions) $\times$ 91 (filter size) independent cluster solutions (cf. Bzdok et al., 2014; Clos et al., 2013; Eickhoff et al., 2016). *K*-means clustering is a non-hierarchical clustering method that uses an iterative algorithm to separate the seed region into a previously selected number of *k* non-overlapping clusters (Forgy, 1965; Hartigan and Wong, 1979). *K*-means aims at minimizing the variance between elements within clusters and maximizing the variance between clusters by first computing the centroid of each cluster and subsequently reassigning voxels to the clusters such that their difference from the nearest centroid is minimal. For each of the 4×91 parcellations, we recorded the best solutions from 100 replications with randomly placed initial centroids. That is, k-means was run 100 times with identical arguments but random centroid initializations (Thirion et al., 2014). Keeping the clustering solution exhibiting lowest voxel-to-centroid distances remedies the tendency for local minima. Please note that a summary estimate across many k-means iterations can consolidate the parcellation estimate, yet cannot guard against this algorithm's risk for local minima.

2.5. Selection of optimal filter range

For each of the 91 filter sizes, the *k*-means procedure thus yielded 4 different solutions for parcellating the VOI into three to six subdivisions. One of the well-known challenges of data clustering in neuroinformatics, and computer science in general, is the choice of an "optimal" cluster solution (so-called "cluster validity problem") (Eickhoff et al., 2015). This problem is further complicated in the current MACM-based parcellation approach because not only the optimal number of clusters *K* had to be determined but also the use of multiple spatial filter sizes. In previous parcellation studies involving MACM and multiple filter sizes, this issue was addressed by averaging *across all filter sizes* (Cieslik et al., 2013). As an improvement of this previous approach, we here used a recently introduced two-step

procedure that involves a first decision on those filter sizes (i.e., the target range) to be included in the final analysis and a second decision on the optimal cluster solution (Bzdok et al., 2014; Clos et al., 2013; Eickhoff et al., 2016). That is, we first examined the properties of each filter size across all cluster solutions and isolated *the most stable range of filter sizes*. These were then submitted to further analysis selecting the number of clusters. The first step was based on the consistency of the cluster assignments for the individual voxels across the different filter sizes and selecting the filter range with the lowest number of deviants, i.e., voxels that were assigned differently as compared to the solution from the majority (mode) of filters. In other words, we identified those filter sizes that reflected solutions most similar to the consensus solution. We then compared the number of *deviant* cluster assignments for parcellation solutions based on different filter sizes. Deviant cluster assignments reflect the number of times a given voxel was assigned to another than the majority cluster, normalized for *K*. The filter size range was set from 100 to 160. This was based on the increase in weighted sum (across all K) of the z-normalized number of deviant voxel assignments before and after these values. That is, at the cut off at $z < -0.5$, only those filter sizes were included where the number of deviants was at least half a standard-deviation below the average number of deviants across all filter sizes. In all subsequent steps, the analysis was thus restricted to the parcellations based on coactivation as estimated from the nearest 100 to 160 experiments.

2.6. Selection of cluster number

We subsequently determined *the optimal solution of k clusters* (restricted to the selected filter sizes as outlined in the last paragraph). This was indicated by majority vote of three different criteria that describe cluster-separation and topological properties of the various cluster solutions.

First, as a topological criterion, we considered the percentage of misclassified voxels (deviants) across filter sizes of a given cluster solution. This criterion indirectly reflects the amount of noise and potentially local effects in the clustering. In particular, the criterion addresses the across-filter stability, that is, the average percentage of voxels for each filter size that were assigned to a different cluster, as compared to the most frequent assignment of these voxels across all filter sizes. Those *k* parcellations were considered good solutions whose percentages of deviants were not increased compared to the *k-1* solution and, in particular, if the subsequent *k+1* solution lead to a higher percentage of deviants.

Second, as another topological criterion, we assessed the percentage of voxels not related to the dominant parent cluster compared to the *K*-1 solution. This measure is related to the hierarchy index (Kahnt et al., 2012) and corresponds to the percentage voxels that are not present in hierarchy, K, compared to the previous K-1 solution. That is, voxels assigned e.g. to the blue cluster in the $K = 3$ solution stemming from a subset of voxels previously assigned to the green cluster (in the $K = 2$ solution) would be excluded if the majority of the blue cluster voxels actually stemmed from the red cluster (in the $K = 2$ solution*). Good solutions* for a given K cluster parcellation were those wherein the percentage of lost voxels was below the median across all possible solutions (i.e., cluster parcellations 3 – 6), where

the respective clustering step resulted in a local minimum and/or the following clustering step featured a maximum in the percentage of lost (hierarchically inconsistent) voxels.

Third, as a cluster-separation criterion, the change in inter- versus intra-cluster distance ratio was computed (Bzdok et al., 2015; Chang et al., 2009). This ratio is defined as the average distance between the cluster centers (i.e., inter-cluster distance) divided by the average distance of a given voxel to its own cluster center (i.e., intra-cluster distance). Increase in this ratio was computed by taking the first derivative. An increased ratio compared to the k-1 solution indicates a better separation of the obtained clusters. Conversely, good solutions do not show a larger inter-cluster distance and a smaller intra-cluster distance in the subsequent k+1 solution.

These three different criteria estimating cluster stability conjointly allowed for an objective, cross-validated identification of the cluster solution with the highest within-cluster homogeneity and between-cluster heterogeneity based on seed-voxel-wise whole brain connectivity.

2.7. Characterization of the clusters: task-dependent connectivity (MACM analysis)

To determine the significant functional connectivity of the derived *clusters*, another meta-analytic connectivity modeling analysis (MACM) was performed. In the first step, we identified all experiments in the BrainMap database that featured at least one focus of activation in a particular cluster derived from the coactivation-based parcellation (CBP). CBP divides a volume of interest into distinct subregions by, first, computing the whole-brain connectivity profile for each individual voxel in the VOI and, second, using the ensuing voxel-wise connectivity profiles to group the VOI voxels such that connectivity is similar for the voxels within a group and different between groups. That is, in contradistinction to the above MACM analyses, we did not select experiments activating at or close to a particular voxel but rather all those that activated in one of the CBP-derived clusters. Next, an ALE meta-analysis was performed on these experiments as described above.

In contrast to the MACM underlying the coactivation-based parcellation, where ALE maps were not thresholded in order to retain the complete pattern of coactivation likelihoods, statistical inference was now performed. To establish which regions were significantly coactivated with a given cluster, ALE scores for the MACM analysis of this cluster were compared to a null-distribution reflecting a random spatial association between experiments with a fixed within-experiment distribution of foci (Eickhoff et al., 2009). This random-effects inference assesses above-chance convergence between experiments, not clustering of foci within a particular experiment. The observed ALE scores from the actual meta-analysis of experiments activating within a particular cluster were then tested against ALE scores obtained under a null-distribution of random spatial association yielding a p-value based on the proportion of equal or higher random values (Eickhoff et al., 2012). The resulting non-parametric p-values were transformed into Z-scores and thresholded at a cluster-level corrected threshold of $p < 0.05$ (cluster-forming threshold at voxel-level $p < 0.001$).

Differences in coactivation patterns between the identified clusters were tested by performing MACM separately on the experiments associated with either cluster and computing the voxel-wise difference between the ensuing ALE maps. All experiments contributing to either analysis were then pooled and randomly divided into two groups of the same size as the two original sets of experiments defined by activation in the first or second cluster (Eickhoff et al., 2011). ALE-scores for these two randomly assembled groups, reflecting the null-hypothesis of label-exchangeability, were calculated and the difference between these ALE-scores was recorded for each voxel in the brain. Repeating this process 10,000 times then yielded a voxel-wise null-distribution on the differences in ALE-scores between the MACM analyses of the two clusters. The 'true' differences in ALE scores were then tested against this null-distribution yielding a p-value for the difference at each voxel based on the proportion of equal or higher differences under label-exchangeability. The resulting p-values were thresholded at p > 0.95 (95% chance of true difference), transformed into Z-scores, and inclusively masked by the respective main effects, i.e., the significant effects in the MACM for the particular cluster.

Finally, we computed the *specific* coactivation pattern for all clusters, that is, brain regions significantly more coactivated with a given cluster than with any of the other ones. This specific cluster-wise coactivation pattern was computed by performing a conjunction analysis over the differences between this cluster and the remaining clusters (see *Results* section for details).

2.8. Characterization of the clusters: task-independent connectivity (RSFC)

Significant cluster-wise whole-brain connectivity was likewise assessed using resting-state correlations as an independent modality of functional connectivity for cross-validation across disparate brain states. RSFC fMRI images were obtained from the Nathan Kline Institute Rockland–sample, which are available online as part of the International Neuroimaging Datasharing Initiative (http://fcon_1000.projects.nitrc.org/indi/pro/nki.html). In total, the processed sample consisted of 10 minutes of resting-state images from 132 healthy participants between 18 and 85 years (mean age: 42.3 ± 18.08 years; 78 male, 54 female) with 260 echo-planar imaging (EPI) images per participant. Images were acquired on a Siemens TrioTim 3T scanner using blood-oxygen-level-dependent (BOLD) contrast [gradient-echo EPI pulse sequence, repetition time (TR) = 2.5 s, echo time (TE) = 30 ms, flip angle = 80°, in-plane resolution=3.0 × 3.0 mm, 38 axial slices (3.0 mm thickness), covering the entire brain]. The first four scans served as dummy images allowing for magnetic field saturation and were discarded prior to further processing using SPM8 (www.fil.ion.ucl.ac.uk/spm). The remaining EPI images were then first corrected for head movement by affine registration using a two-pass procedure. The mean EPI image for each participant was spatially normalized to the MNI single-subject template (Holmes et al., 1998) using the 'unified segmentation' approach (Ashburner and Friston, 2005). The ensuing deformation was then applied to the individual EPI volumes. Finally, images were smoothed by a 5-mm FWHM Gaussian kernel to improve signal-to-noise ratio and account for residual anatomical variations.

The time-series data of each individual seed voxel were processed as follows (Fox et al., 2009; Weissenbacher et al., 2009): In order to reduce spurious correlations, variance that could be explained by the following nuisance variables was removed: (i) The six motion parameters derived from the image realignment, (ii) the first derivative of the realignment parameters, and (iii) mean gray matter, white matter, and CSF signal per time point as obtained by averaging across voxels attributed to the respective tissue class in the SPM 8 segmentation (Reetz et al., 2012). All of these nuisance variables entered the model as first- and second-order terms (Jakobs et al., 2012). Data were then band-pass filtered preserving frequencies between 0.01 and 0.08 Hz since meaningful resting-state correlations will predominantly be found in these frequencies given that the BOLD-response acts as a low-pass filter (Biswal et al., 1995; Fox and Raichle, 2007).

To measure cluster-wise task-independent connectivity, time courses were extracted for all gray-matter voxels of a given cluster. The cluster time course was then expressed as the first eigenvariate of these voxels' time courses. Pearson correlation coefficients between the time series of the CBP-derived LPL clusters and all other gray-matter voxels in the brain were computed to quantify RSFC. These voxel-wise correlation coefficients were then transformed into Fisher's Z-scores and tested for consistency across participants using a random-effects, repeated-measures analysis of variance. The main effect of connectivity for individual clusters and contrasts between them were tested using the standard SPM8 implementations with the appropriate non-sphericity correction. The results of these random-effects analyses were cluster-level corrected for multiple comparisons at $p < 0.05$ (cluster-forming threshold at voxel-level: $p < 0.001$), analogous to the MACM-based difference analysis. The specific resting-state correlations for a given cluster were then computed by performing a conjunction analysis across the differences between a given cluster and the remaining ones, analogous to the MACM-based cluster analyses above.

2.9. Characterization of the clusters: conjunction across connectivity types and clusters

To specify brain regions showing task-dependent and task-independent functional connectivity with the derived clusters in the LPL, we performed a conjunction analysis of the MACM and RSFC results using the strict minimum statistics (Nichols et al., 2005). Brain regions connected with *individual clusters* across both connectivity measures were characterized by computing the intersection (i.e., AND-conjunction) of the (cluster-level family-wise-error-corrected) connectivity maps from the two connectivity analyses detailed above. In this way, each LPL cluster was associated with a network of brain regions that are congruently connected to that cluster across two disparate brain states, i.e., mental operations in a task-focused and task-free setting.

2.10. Characterization of the clusters: function (functional decoding)

Finally, the identified clusters were individually submitted to functional decoding (Amft et al., 2014; Balsters et al., 2014; Muller et al., 2013). Note that this functional characterization constitutes a post-hoc procedure that is subsequent to and independent of the connectivity analyses. The functional characterization was based on the BrainMap meta-data that describe each neuroimaging experiment included in the database. Behavioral domains code the mental processes isolated by the statistical contrasts (Fox et al., 2005) and comprise the

main categories cognition, action, perception, emotion, and interoception, as well as their related sub-categories. Paradigm classes categorize the specific task employed (see http://brainmap.org/scribe/ for the complete BrainMap taxonomy).

Forward inference on the functional characterization then tests the probability of observing activity in a brain region given knowledge of the psychological process, whereas *reverse inference* tests the probability of a psychological process being present given knowledge of activation in a particular brain region (Varoquaux and Thirion, 2014; Yarkoni et al., 2011). In the forward inference approach, a cluster's functional profile was determined by identifying taxonomic labels for which the probability of finding activation in the respective cluster was significantly higher than the a priori chance (across the entire database) of finding activation in that particular cluster. Significance was established using a binomial test ($p < 0.05$). That is, we tested whether the conditional probability of activation given a particular label [P(Activation|Task)] was higher than the baseline probability of activating the region in question per se [P(Activation)]. In the reverse inference approach, a cluster's functional profile was determined by identifying the most likely behavioral domains and paradigm classes given activation in a particular cluster. This likelihood P(Task|Activation) can be derived from P(Activation|Task) as well as P(Task) and P(Activation) using Bayes' rule. Significance was then assessed by means of a chi-square test ($p < 0.05$). In sum, forward inference assessed the probability of activation given a psychological term, while reverse inference assessed the probability of a psychological term given activation.

In the context of quantitative functional decoding, it is important to appreciate that this approach aims at relating defined psychological tasks to the examined brain regions instead of claiming "a unique role" of a brain region for any psychological task (Poldrack, 2006; Yarkoni et al., 2011). Put differently, an association of task X to brain region Y obtained in these analyses does not necessarily imply that neural activity in region Y *is limited to* task X.

2.11. Anatomical localization

The SPM Anatomy Toolbox (Eickhoff et al., 2007; Eickhoff et al., 2005) was used to allow for investigator-independent anatomical localization of imaging results. By means of maximum probability map (MPM), activation clusters were automatically assigned to the most likely cytoarchitectonic area. MPMs are drawn from earlier microscopic investigations, including the inter-subject variability and aided by algorithmic definition of micro-anatomial borders of brain areas (Zilles and Amunts, 2010). Please note that not all activation clusters could thus be assigned to a cytoarchitectonic map.

3. Results

3.1. Cluster number

Several cluster validity metrics (cf. Eickhoff et al., 2015) were applied to weigh the various cluster solutions for the parietal VOI against each other (Figure 3). First, as a topological criterion, the percentage of misclassified voxels across filter sizes was lowest for solutions up to four clusters. This indicated that low cluster numbers exhibited the least noise across

the different filter sizes. Second, as another topological criterion, the percentage of voxels not related to the dominant parent cluster was lower in the four-cluster solution than for solutions with more clusters. Dividing the parietal VOI into four clusters thus contained relatively few re-grouped voxels and therefore high continuity with their dominant parent cluster from the k-1 solution. Third, change of 'inter-cluster/intra-cluster ratio', another cluster-separation criterion, was higher for four clusters comparing to the three- and five-cluster solutions. This indicated that the four-cluster solution isolated each cluster well from the remaining ones. The four different measures of clustering quality thus unequivocally advocated the four-cluster solution as the most neurobiologically meaningful division model of the parietal VOI (Figure 4).

3.2. Cluster topography

Although the four-cluster solution emerged as the best-fitting model, it is instructive to consider the neighboring cluster solutions and their relations. In the three-cluster solution (Figure 2, top row), dorsal aspects of the VOI were separated into a single cluster (cytoarchitectonically assigned to hIP1, hIP3, and 7A; Choi et al., 2006), while ventral aspects of the VOI were separated into a rostro-ventral (most likely related to Wernicke's area, no cytoarchitectonic assignment) and a red caudo-ventral (cytoarchitectonically assigned to PGa and PGp; Caspers et al., 2006) cluster. In the four-cluster solution (Figure 2, middle row), the former dorsal cluster was further subdivided into a bigger green rostro-medial (cytoarchitectonically assigned hIP2, hIP3, and 7A; Choi et al., 2006; Scheperjans et al., 2008) and a smaller caudo-lateral (cytoarchitectonically assigned to hIP1, hIP3, and PGa; Caspers et al., 2008; Choi et al., 2006) cluster. In the five-cluster solution (Figure 2, bottom row), the former cluster was further subdivided into a medial (cytoarchitectonically assigned to hIP1, hIP3, and 7A; Choi et al., 2006; Scheperjans et al., 2008) and a lateral (cytoarchitectonically assigned to hIP1 and PGa; Caspers et al., 2008; Scheperjans et al., 2008) cluster.

Note that k-means clustering was here applied independently several times to the same VOI. This procedure does not enforce hierarchically consistent cluster solutions (Jain, 2010; Jain et al., 1999). Nevertheless, the rostro-ventral and caudo-ventral clusters emerged independently with consistent topography in all three clustering analyses. This means that the regional heterogeneity in the whole-brain connectivity was more prominent for these clusters than for the clusters emerging from the green cluster. In other words, *the two clusters in the ventral VOI capture a more distinct connectional-functional segregation than the later emerging clusters in the dorsal VOI* (Passingham et al., 2002). We will therefore focus on the four-cluster solution in this paper.

3.3. Individual cluster connectivity

We first assessed the cluster-level corrected meta-analytic coactivations (MACM) and resting-state functional connectivity (RSFC) of each LPL cluster individually (Figure 5, upper row). In MACM analyses, cluster 1 featured bilateral connectivity to the inferior parietal lobe (cytoarchitectonically assigned to PGa, PF, and PFm; Caspers et al., 2006), the superior/middle temporal gyrus (STG, MTG), superior temporal sulcus (STS), inferior frontal gyrus (IFG; cytoarchitectonially assigned to BA44/45; Amunts et al., 1999), anterior

insula (AI), mid-cingulate gyrus (MCC)/supplementary motor cortex (SMA, cytoarchitectonically assigned to BA6), posterior cingulate cortex (PCC), and thalamus. Furthermore, cluster 1 was connected to the right precuneus. The cluster-level corrected RSFC of cluster 1 (Figure 5, middle row) featured the same set of connectivity targets, except for significant connectivity to the thalamus, with higher overall connectivity strengths. This was formally confirmed by the conjunction analysis between MACM and RSFC connectivity of cluster 1 (Figure 5, lower row).

Cluster 2 featured bilateral connectivity to the inferior parietal lobe (cytoarchitectonically assigned to PGa, PGp, and PFm), ventromedial-, frontopolar, and dorsomedial prefrontal cortex (vmPFC, FP, dmPFC), extending into the anterior ACC (rACC), PCC/precuneus, and MTG, extending into the left STS. Cluster 2 was also connected to the left IFG (extending into the AI), hippocampus (cytoarchitectonically assigned to CA; Amunts et al., 2005), extending into the amygdala, as well as superior frontal gyrus and dorsolateral prefrontal cortex (dlPFC). This connectivity profile was absent for the respective right hemispheric regions. These connectivity targets were confirmed by individual RSFC and its conjunction with MACM results. Yet, cluster 2 showed also significant RSFC to the right MTG.

Clusters 3 and 4 showed highly similar connectivity patterns, although regionally differing in connectivity strength. Both clusters were connected to the bilateral inferior parietal lobe and intraparietal sulcus (IPS) (cytoarchitectonically assigned to hIP, PGa, and 7A; Choi et al., 2006), dlPFC, IFG (cytoarchitectonically assigned to BA44/45), AI, MCC/SMA (cytoarchitectonically assigned to BA6), thalamus, precuneus, primary visual cortex, and cerebellum (not shown). Both clusters were further connected to the left MTG. In individual and conjunction RSFC analysis, the significant connectivity targets of cluster 3 and 4 were confirmed by generally stronger correlation. Yet, cluster 3 and 4 also showed RSFC to the bilateral inferior temporal gyrus. Additionally, cluster 3 showed additional RSFC to the PCC and precuneus, while cluster 3 did not show the thalamic connectivity observed in MACM.

3.4. Specific cluster connectivity

Given the overlap between the connectivity profiles of the LPL clusters, we investigated parts of the brain that were more strongly connected to a given cluster than the respective three other clusters (Figure 6). To this end, we isolated the brain regions that were selectively connected with a given cluster in contrast to all remaining clusters. For instance, to characterize the specific cluster connectivity of cluster 1, we computed the AND conjunction across the three difference maps (clusters 1 - clusters2), (cluster 1 – cluster 3), and (clusters 1 – cluster 4). This procedure removed connectivity of cluster 1 that was shared with clusters 2, 3, and 4. This is because any voxel that is deemed to reflect *specific* connectivity of a given cluster had been determined to be statistically more associated with that cluster in three separate difference analyses with the respective three other clusters.

According to MACM, cluster 1 featured highest connectivity strength to the bilateral STG (coinciding with Wernicke's area on the left side), STS, IFG, as well as aspects of the inferior parietal lobe (cytoarchitectonically assigned to PF/PFm). In the left hemisphere, cluster 1 was also specifically connected to the AI. These specific connectivity targets were confirmed by RSFC. Additionally, cluster 1 feature highest RSFC to the MTG, temporal

pole (TP), and mid/posterior cingulate cortex. The conjunction across specific MACM and RSFC corroborated the specific MACM profile of cluster 1, except for the left AI and IFG.

Cluster 2, according to MACM, demonstrated the highest connectivity strength to the bilateral vmPFC/FP/dmPFC (Bzdok et al., 2013a), extending into the rACC, PCC, as well as aspects of the inferior parietal lobe (cytoarchitectonically assigned to PGp). Specific connectivity in the left hemisphere was observed in the SFG and MTG. Notably, cluster 2 yielded the most widespread selective connectivity to highly associative brain regions among all four clusters. RSFC confirmed these specific connectivities by conjunction analysis and showed additional distributed results by individual analysis in the midcingulate, medial temporal, visual, and anterior-cingulate regions.

Cluster 3 featured highest MACM coupling with the bilateral IPS (cytoarchitectonically assigned to hIP1) and anterior aspects of dlPFC. Specific connectivity in the left hemisphere was observed in left inferior temporal gyrus (IFG) and anterior aspects of MCC/SMA. Individual and conjunction RSFC analysis confirmed this set of regions. Yet, a part of the PCC and the right IFG were only revealed by specific RSFC.

Cluster 4 featured highest MACM connectivity to bilateral superior parietal lobe (cytoarchitectonically assigned to area 7A), posterior aspects of MCC/SMA (cytoarchitectonically assigned to BA6), and posterior aspects of dlPFC, as well as AI, primary visual cortex (including fusiform gyrus), and cerebellum (not shown). Indeed, specific RSFC confirmed this entire set of regions by conjunction analysis, except for the visual cortex.

3.5. Functional decoding of clusters

We performed quantitative functional decoding by testing for BrainMap meta-data terms associated with activation in each cluster (Figure 7). For the sake of robustness, the description of functional associations will be concentrated on taxonomic associations that were determined to be statistically significant in both forward and reverse inference analyses. Note that the functional decoding analysis represents a descriptive post-hoc analysis of the functional profile of *individual clusters* rather than a direct comparison *between different clusters*.

Importantly, both cluster 1 and 2 were congruently (i.e., across forward and reverse inference) functionally associated with general social cognition processing, including theory of mind, as well as semantic processing. Cluster 2 was further congruently functionally associated with explicit memory retrieval and episodic memory retrieval.

Both cluster 3 and 4 were congruently associated with working memory and general cognitively demanding tasks, including delayed match to sample and n-back tasks, spatial processing, including mental rotation, as well as number processing, including counting. Only cluster 3 was congruently associated with Wisconsin card sorting test, while only cluster 4 was further congruently associated with visual processing, saccade generation, and attentional tasks, including stroop experiments.

4. Discussion

We here used connectivity-based parcellation to investigate the functional heterogeneity of the left parietal lobe during social-cognition and language performance. We targeted the question whether both functions engage the same or different anatomical subregions within the left parietal lobe. Driven by regional differences in coactivation patterns derived from hundreds of neuroimaging studies archived in the BrainMap database (Fox and Lancaster, 2002), the VOI in the left parietal lobe was segregated into 3 to 6 clusters. Across clustering analyses, clusters emerging in the ventral versus dorsal VOI were more consistent. The four-cluster solution was identified as the most neurobiologically meaningful subdivision of the present VOI. As the first main finding, two clusters in the inferior VOI were significantly associated with both social cognitive and language processes. This suggests that the inferior parietal lobe is a convergence zone of social cognitive and language processing. As the second main finding, connectivity and functional decoding analyses indicated a rostro-versus caudo-ventral distinction of inferior VOI clusters (Figure 2, in blue and red), related to lower- versus higher-level aspects, respectively, of both social and language processes (see below for details). In contrast, clusters that emerged in the superior VOI (Figure 2, in orange) were connectionally and functionally related to domain-general attention and working-memory processes.

On a methodological note, we relied on a data-guided meta-analytically-defined seed region for target volume definition to make a minimum of a-priori assumptions from neuroanatomical nomenclature or cognitive theory. Consequently, the VOI definition was functionally, rather than anatomically, motivated. *This was accounted for by the word choice "LPL" and explains why this VOI exceeds the parietal lobe proper to include adjacent parts of the posterior superior temporal gyrus and posterior temporal sulcus* (cf. Bzdok et al., 2013b; Mars et al., 2012).

4.1. Specific connectivity profiles of the four-cluster solution

The rostro-ventral cluster 1 (blue) exhibited *specific* connectivity (i.e., connectivity that is stronger with cluster 1 than any other cluster in the LPL VOI) with the bilateral superior temporal gyrus and sulcus, inferior frontal gyrus, and regions in the left parietal lobe, as well as functional associations with general social cognitive and semantic processing. These areas have previously been associated with general aspects of task processing and stimulus-response processing in social cognition and language tasks (e.g., non-story based theory of mind processes, see Mar, 2011 for meta-analysis). Note that cluster 1 could not be assigned to any cytoarchitectonically defined region. This might explain the inconsistent labeling of this region in previous literature (see introduction and below).

In contrast to cluster 1, the caudo-ventral cluster 2 (red) was *specifically* connected with the bilateral inferior parietal lobe, ventro- and dorsomedial prefrontal cortex (extending into the neighboring anterior cingulate cortex) and the posterior cingulate cortex, and left superior frontal gyrus and middle frontal gyrus. Functional decoding analysis revealed associations with general social cognitive, semantic and memory processing. Previous studies suggested that the above described regions subserve high-level associative functions, including the default mode of brain function (Buckner et al., 2008; Raichle et al., 2001). Accordingly, the

observed connectivity profile for cluster 2 converges with a previous resting-state correlation study that reported increased task-independent connectivity for a similarly located region with the default-mode network (Uddin et al., 2011). It was suggested that the default mode network maintains stimulus-independent thoughts or mind wandering (Konishi et al., 2015; Raichle et al., 2001; Weissman et al., 2006). It may set the stage for self-projection and scene construction in the constant switching between interoceptive and exteroceptive mind states (Buckner and Carroll, 2007; Li et al., 2015; Mars et al., 2013). Cytoarchitectonically, cluster 2 was here assigned to area PGa and PGp (Bzdok et al., 2013b; Caspers et al., 2006). While these regions are often labeled as either "temporo-parietal junction" or "angular gyrus" in neuroimaging studies, their proper anatomical borders are subject to debate (Decety and Lamm, 2007; Seghier, 2013).

The remaining two clusters in the dorsal VOI were characterized by highly similar connectivity profiles. The rostro-medial cluster 3 (orange) featured *specific* connectivity to bilateral IPS and anterior portions of the dorsolateral prefrontal cortex as well as left middle temporal gyrus / inferior temporal sulcus and anterior mid-cingulate cortex / supplementary motor area. Finally, the caudo-lateral aspect of the dorsal VOI (green cluster 4) was connected to extended portions of the bilateral IPS, posterior supplementary motor area, and posterior dorsolateral prefrontal cortex / primary motor cortex, cerebellum, anterior insula, and primary visual cortex, including the right fusiform gyrus. Notably, cluster 3 and 4 featured connections to areas previously associated with general cognitive control processes (i.e., bilateral IPS, SMA / MCC and insula (Clos et al., 2013; Dehaene et al., 2003; Dosenbach et al., 2006; Seeley et al., 2007)). This is consistent with these clusters' present functional associations such as working memory, n-back, spatial processing and number processing tasks. Cytoarchitectonically, the green cluster 3 was assigned to (cytoarchitectonically assigned hIP2, hIP3, and 7A; Choi et al., 2006; Scheperjans et al., 2008). The orange cluster 4 was assigned to neighboring regions (cytoarchitectonically assigned to hIP1, hIP3, and PGa; Caspers et al., 2008; Choi et al., 2006).

4.2. Left inferior parietal lobe engagement in social cognition and language: Evidence for distinct functional modules

To the best of our knowledge, no previous neuroimaging study has aimed at the dissociation between high-level social and language processes in the LPL area (cf. Kobayashi et al., 2007; Straube et al., 2010). This suggests that these cognitive processes might be too closely entangled to be successfully teased apart by contemporary MRI technology and available neuroimaging repositories. It is thus enticing to speculate that both social and language functions might rely on identical neural mechanisms for problem solving. This notion is supported by our observation of a strongly overlapping functional association with social cognition and semantic processes in cluster 1 and 2. Indeed, functional decoding analyses revealed that clusters 1 and 2 were *congruently* (i.e., across forward and reverse functional inference) associated with social cognition and semantics. *It is hence possible that neural tissue in cluster 1 and 2 solves computational problems that are shared by, but not specific to, social or linguistic processing problems.* In fact, a similar interpretation was proposed for the right temporo-parietal junction (Decety and Lamm, 2007; Kobayashi et al., 2006).

However, cluster 2 (but not 1) was additionally associated with cognitively more complex and demanding tasks such as episodic or explicit memory retrieval and syntactic processing. Episodic and explicit memory retrieval strongly draws on complex semantic processing and contributes to social cognitive processes (see section 4.4.). Syntactic processing, on the other hand, is a core language process that is closely intermingled with semantic processing. It refers to the hierarchical sequencing of words and their meanings (Price, 2010) and is mandatory for sentence processing in both social cognitive and language tasks. Together, this favors a more specialized contribution of cluster 2 to high-level social cognitive and language functions, including semantic integration and sentence processing. Hence, we propose distinct functional modules within the LPL, with the rostro-ventral cluster 1 (blue) being engaged in lower-level aspects of stimulus processing and external task response (i.e., perception-action cycles) and the caudo-ventral red cluster being engaged in complex semantic computations. This notion is supported by our finding that cluster 1 showed a more bilateral connectivity pattern, while the functional connectivity profile of cluster 2 was more strongly left-lateralized (Binder et al., 2009). This further converges with recent functional-anatomical models of language (e.g., Hickok and Poeppel, 2004; Hickok and Poeppel, 2007). These models favor a bilateral organization of low-level speech functions and early cortical processes of speech perception, which engage, among others, the posterior STG (coinciding with our blue cluster 1). In contrast, more complex conceptual linguistic functions are proposed to be more strongly left-lateralized (see also Hickok, 2009).

The notion of distinct functional modules was also proposed for the right TPJ area (Bzdok et al., 2013b; Mars et al., 2011; Schurz et al., 2014). Consequently, the here observed rostro-caudal increase in cognitive complexity in the left-hemispheric inferior parietal lobe might mirror a similar shift from more rostral lower-order to more caudal complex computation in the right-hemispheric inferior parietal lobe (Caspers et al., 2011).

This contention goes hand-in-hand with recent models of social cognition. For instance, Schaafsma and colleagues (2015) suggested that social cognition can be subdivided in two processing streams. A rapid, automatic processing stream might not require verbal competence. In contrast, a slower, deliberative verbal form is featured when we consciously reflect about social cognitive processes. Accordingly, a recent meta-analysis provided evidence for an involvement of a more anterior region in the left pSTG / STS (coinciding with the blue cluster 1) in non-verbal and non-story theory of mind processing. In contrast, a more posterior region in the left angular gyrus / temporal parietal junction (coinciding with the red cluster 2) was associated with theory of mind stories that hinge on verbal processing analysis (Mar, 2011). A functional-anatomical dissociation of low-level vs. higher level processing facets would be further supported by several previous neuroimaging studies on language (Vigneau et al., 2006). These authors suggested that the processing of verbal material follows a rostro-caudal information flow in left temporo-parietal regions. Low-level auditory semantic analyses were associated with the posterior portion of the pSTG / STS (coinciding with blue cluster 1), while a region in the angular gyrus of the LPL (coinciding with red cluster 2) would be engaged in semantic analysis. The present and previous results thus converge to social cognition and language processes functionally overlapping and likely recruiting very similar neural networks with different LPL nodes as a function of task complexity.

4.3. Contributions of cluster 1 to social cognition and language: low-level processing facets

With respect to the precise functions of the blue cluster 1, previous studies associated a similarly located area in the pSTG / STS with hierarchically lower social processes like gaze (Calder et al., 2002) or the observation of whole-body motion or unexpected body motion (Van Overwalle, 2009). This author argued that these processes likely reflect an orientation response in line with the action or attention of the observed actor. Accordingly, increased task-related activity of the left pSTG / STS was also found during person vs. object processing (Abraham et al., 2008), (non-verbal) theory of mind cartoons vs. non-theory of mind cartoons (Vollm et al., 2006) or false beliefs vs. false photo tasks (Aichhorn et al., 2009). It was suggested that the false-belief task might simply be more executively demanding than the photo task. This contention assumed that false-belief tasks require the reconciliation of a discrepancy between someone's belief and the current state of the world (Cohen et al., 2014). Hence, these contrasts might express domain-general executive demanding processes rather than domain-specific social cognitive processes (Sabbagh et al., 2006).

It is important to appreciate that our cluster 1 is located in the "classical semantic" Wernicke's area in the pSTG (Geschwind, 1970). Its neuroanatomical borders remain cytoarchitectonically under-researched. The pSTG / STS was previously associated with pre-lexical speech and covert articulation (Price, 2010) or the processing of syntactically correct but meaningless pseudo-words with low semantic demands (Hickok et al., 2003). Virtual lesions induced by transcranial magnetic stimulation (TMS) (Andoh et al., 2006) favored a pSTG contribution to auditory working memory and sound representations, consistent with our line of interpretation for cluster 1 above. Moreover, anodal transcranial direct current stimulation over this area facilitated novel object learning of non-words, probably via enhancing phonological retrieval and working memory (Fiori et al., 2011; Meinzer et al., 2014).

4.4. Contributions of cluster 2 to social cognition and language: complex task functions

In contrast to cluster 1, the red cluster 2 was associated with more complex task functions, such as explicit memory processing, in our study. This ties in with previous studies assigning this region a role in semantic working memory (Vigneau et al., 2006) or autobiographical memory (Spreng et al., 2009). Particularly, autobiographical memory inevitably draws on self-projection, mentalizing, and mental-scene construction. Of note, these mental imagery processes require semantic processing and are associated with increased activation of the default-mode network, including the angular gyrus (Nelson et al., 2010; Schacter et al., 2007). Similarly, several studies demonstrated increased task-related activity of the left angular gyrus / temporo-parietal junction during theory of mind stories as compared with unlinked sentences or stories that do not require theory of mind (Fletcher et al., 1995; Kobayashi et al., 2007). Moreover, the social cognition literature provides evidence for a contribution of this area to de-novo generation of meaning representations and contextual construction during event elaboration when participants had to recall past events or imagine future events (Addis et al., 2007). Please appreciate that these processes are very likely to draw on semantic knowledge retrieval (Binder et al., 1999).

Language studies have further demonstrated that stroke-induced lesions of the angular gyrus (overlapping our cluster 2) impaired processing of passive reversible sentences (e.g., "the niece was kicked by the father") and complex object cleft constructions (e.g., "It was the niece that the father kicked") (Newhart et al., 2011). This suggests a role of the angular gyrus in complex working memory and syntax. Hence, this region might represent an amodal gateway that mediates reciprocal interactions between the sensory processing of words and objects and the symbolic association of their meanings (Vigneau et al., 2006). A high-level integrative semantic function of the angular gyrus is supported by presurgical electrode recordings (Lien et al., 2014) and neurological lesion studies (Hart and Gordon, 1990). Moreover, temporary perturbation of angular gyrus function impaired performance on semantic category judgments and the processing of acoustically degraded sentences with high-predictable endings (Sliwinska et al., 2014). Taken together, present and previous evidence converges to a core contribution of intact angular gyrus function (coinciding with red cluster 2) to semantic processing on the word and sentence level.

4.5. Contributions of cluster 3 and 4 to social cognition and language: General aspects of task processing

We found evidence for two additional functionally distinct modules in the dorsal VOI (i.e., cluster 3 and 4). Both clusters revealed highly similar connectivity profiles and were related to general aspects of task-maintenance required for successful social cognition and language performance (Corbetta et al., 2008; Hartwigsen et al., 2014). These processes include domain-general functions such as attention, low-level working memory, executive selection and perception, which are likely recruited for tasks outside the core domain-specific social cognitive or language functions. We would thus argue that the reported activation of the respective regions in fMRI studies of social cognition and language most likely reflects general cognitive processing facets that do not necessarily indicate a causal contribution to the core facets of both functions.

Indeed, previous neuroimaging studies have reported increased activation of an area in the left anterior intraparietal sulcus (aIPS) (overlapping with the orange cluster 3) for spatial working memory and attention tasks as well as symbolic and non-symbolic locations (Zago et al., 2008), spelling (Bitan et al., 2005) or phonological working memory processes during language and n-back tasks (Awh et al., 1996; Smith et al., 1998). Ossmy and colleagues (2014) suggested that the aIPS contributes to reading by processing the relative letter positions. A role of the aIPS in more general processes required for higher-level cognitive functions is further supported by previous virtual lesion studies (Whitney et al., 2012). Hence, perturbation of the aIPS disrupted both semantic and non-semantic control demands, indicating that this region plays a wider role in cognition beyond the semantic domain, including the processing of perceptual task demands with low conceptual content (Jefferies and Lambon Ralph, 2006). Accordingly, increased neural activity in the aIPS region was previously associated with a general increase in the cognitive load and task difficulty (Dosch et al., 2009; Vogeley et al., 2004).

In accordance with the results from our functional decoding analyses, a region overlapping with the green cluster 4 was associated with attentional processes during social cognition

tasks (Addis et al., 2009) or visuo-spatial processes during navigation tasks (Spreng et al., 2009), as well as action observation and imitation (Caspers et al., 2010). A contribution of cluster 4 to attention-related and executive functions was further supported by several neuroimaging studies that found increased activity in this area when participants had to cooperate with either human or computer partners in an economic game (Rilling et al., 2004). Both situations require strong risk-benefit calculations and executive processes that flank more genuine cooperative and social processes. Indeed, the study by Rilling and collaborators (2004) reported stronger activation in this area for the cooperation with a computer than a human partner, which might reflect allocation of attentional resources when the subjects were trying to elucidate the computer's strategy and the optimal response to it.

4.6. The role of the left vs. right parietal lobe in social cognition and language

More generally, the present study focused on the *left* PL. This is because it is the most relevant macroscopical intersection between social and language processes (see Binder et al., 2009; Mar, 2011). On the one hand, high-level social cognition is well known to modulate neural activity in a widespread network including the bilateral PL. Indeed, previous studies demonstrated that the *right* inferior PL also plays a key role in social cognition tasks (Bzdok et al., 2013b; Decety and Lamm, 2007; Koster-Hale et al., 2013). Language functions, on the other hand, typically modulate neural activity in strongly left-lateralized brain regions. It was argued that the reported activation of the right inferior PL during social cognition tasks might be of particular relevance for reflecting on another person's true and false beliefs (Dohnel et al., 2012; Kobayashi et al., 2006; Saxe and Kanwisher, 2003). We would thus argue that the shared subprocesses across social cognition and semantic processing are most closely associated with intact *left* inferior parietal lobe function.

5. Conclusions

Present and previous findings converge to three conclusions. First, theory of mind and language related processing facets are unlikely to be clearly dissociable in the LPL based on large quantities of fMRI measurements. More specifically, any cluster discovered in the parietal VOI that turned out to be congruently functionally associated with social tasks (i.e., the blue cluster 1 and the red cluster 2) also featured significant functional association with language tasks, and vice versa. This concurs with the closely intertwined relationship between the development of social cognitive and language capabilities in children (Heyes and Frith, 2014), human cultural evolution (Tomasello, 1999), the anthropology of contemporary human societies (Mesoudi et al., 2006), and general brain physiology (Binder et al., 2009; Bzdok et al., 2012).

Second, while cluster 1 and 2 were both congruently associated with social-cognitive and language tasks, our data provide evidence for distinct functional modules in the rostro-caudal LPL. Cluster 1 might predominantly subserve lower-level processing facets in social cognition and language and cluster 2 might be more engaged in higher-level facets of these processes. Accordingly, only cluster 2 showed specific connectivity to the entirety of the default-mode network and additional functional association with advanced cognitive processes, including explicit and episodic memory recall.

Third, the orange cluster 3 and green cluster 4 showed neither connectional nor functional evidence for a domain-specific involvement in either social or language cognitive processes. Rather, the observed connectivity patterns and functional task associations of these two clusters can be explained by involvement in general-purpose visual, spatial and attentional processes. These appear to be frequently co-recruited by social and language cognition in the intact human brain.

Acknowledgments

References

Abraham A, Werning M, Rakoczy H, von Cramon DY, Schubotz RI. Minds, persons, and space: an fMRI investigation into the relational complexity of higher-order intentionality. Consciousness and cognition. 2008; 17:438–450. [PubMed: 18406173]

Addis DR, Pan L, Vu MA, Laiser N, Schacter DL. Constructive episodic simulation of the future and the past: distinct subsystems of a core brain network mediate imagining and remembering. Neuropsychologia. 2009; 47:2222–2238. [PubMed: 19041331]

Addis DR, Wong AT, Schacter DL. Remembering the past and imagining the future: common and distinct neural substrates during event construction and elaboration. Neuropsychologia. 2007; 45:1363–1377. [PubMed: 17126370]

Aichhorn M, Perner J, Weiss B, Kronbichler M, Staffen W, Ladurner G. Temporo-parietal junction activity in theory-of-mind tasks: falseness, beliefs, or attention. J Cogn Neurosci. 2009; 21:1179–1192. [PubMed: 18702587]

Amft M, Bzdok D, Laird A, Fox P, Eickhoff S. Definition and characterization of the extended default mode network. Brain Structure & Function. 2014 in press.

Amunts K, Kedo O, Kindler M, Pieperhoff P, Mohlberg H, Shah NJ, Habel U, Schneider F, Zilles K. Cytoarchitectonic mapping of the human amygdala, hippocampal region and entorhinal cortex: intersubject variability and probability maps. Anat Embryol (Berl). 2005; 210:343–352. [PubMed: 16208455]

Amunts K, Schleicher A, Burgel U, Mohlberg H, Uylings HB, Zilles K. Broca's region revisited: cytoarchitecture and intersubject variability. The Journal of comparative neurology. 1999; 412:319–341. [PubMed: 10441759]

Andoh J, Artiges E, Pallier C, Riviere D, Mangin JF, Cachia A, Plaze M, Paillere-Martinot ML, Martinot JL. Modulation of language areas with functional MR image-guided magnetic stimulation. NeuroImage. 2006; 29:619–627. [PubMed: 16168674]

Ashburner J, Friston KJ. Unified segmentation. NeuroImage. 2005; 26:839–851. [PubMed: 15955494]

Awh E, Jonides J, Smith EE, Schumacher EH, Koeppe RA, Katz S. Dissociation of storage and rehearsal in working memory: PET evidence. Psychol Sci. 1996; 7:25–31.

Balsters JH, Laird AR, Fox PT, Eickhoff SB. Bridging the gap between functional and anatomical features of cortico-cerebellar circuits using meta-analytic connectivity modeling. Hum Brain Mapp. 2014; 35:3152–3169. [PubMed: 24142505]

Binder JR, Desai RH. The neurobiology of semantic memory. Trends in cognitive sciences. 2011; 15:527–536. [PubMed: 22001867]

Binder JR, Desai RH, Graves WW, Conant LL. Where is the semantic system? A critical review and meta-analysis of 120 functional neuroimaging studies. Cerebral cortex. 2009; 19:2767–2796. [PubMed: 19329570]

Binder JR, Frost JA, Hammeke TA, Bellgowan PS, Rao SM, Cox RW. Conceptual processing during the conscious resting state: a functional MRI study. Journal of cognitive neuroscience. 1999; 11:80–93. [PubMed: 9950716]

Biswal B, Yetkin FZ, Haughton VM, Hyde JS. Functional connectivity in the motor cortex of resting human brain using echo-planar MRI. Magnetic resonance in medicine : official journal of the Society of Magnetic Resonance in Medicine / Society of Magnetic Resonance in Medicine. 1995; 34:537–541.

Bitan T, Booth JR, Choy J, Burman DD, Gitelman DR, Mesulam MM. Shifts of effective connectivity within a language network during rhyming and spelling. J Neurosci. 2005; 25:5397–5403. [PubMed: 15930389]

Buckner RL, Andrews-Hanna JR, Schacter DL. The brain's default network: anatomy, function, and relevance to disease. Annals of the New York Academy of Sciences. 2008; 1124:1–38. [PubMed: 18400922]

Buckner RL, Carroll DC. Self-projection and the brain. Trends in cognitive sciences. 2007; 11:49–57. [PubMed: 17188554]

Bzdok D, Heeger A, Langner R, Laird A, Fox P, Palomero-Gallagher N, Vogt B, Zilles K, Eickhoff S. Subspecialization in the human posterior medial cortex. NeuroImage. 2014 in press.

Bzdok D, Heeger A, Langner R, Laird AR, Fox PT, Palomero-Gallagher N, Vogt BA, Zilles K, Eickhoff SB. Subspecialization in the human posterior medial cortex. NeuroImage. 2015; 106:55–71. [PubMed: 25462801]

Bzdok D, Langner R, Schilbach L, Engemann DA, Laird AR, Fox PT, Eickhoff SB. Segregation of the human medial prefrontal cortex in social cognition. Frontiers in human neuroscience. 2013a; 7:232. [PubMed: 23755001]

Bzdok D, Langner R, Schilbach L, Jakobs O, Roski C, Caspers S, Laird AR, Fox PT, Zilles K, Eickhoff SB. Characterization of the temporo-parietal junction by combining data-driven parcellation, complementary connectivity analyses, and functional decoding. NeuroImage. 2013b; 81:381–392. [PubMed: 23689016]

Bzdok D, Schilbach L, Vogeley K, Schneider K, Laird AR, Langner R, Eickhoff SB. Parsing the neural correlates of moral cognition: ALE meta-analysis on morality, theory of mind, and empathy. Brain Struct Funct. 2012; 217:783–796. [PubMed: 22270812]

Calder AJ, Lawrence AD, Keane J, Scott SK, Owen AM, Christoffels I, Young AW. Reading the mind from eye gaze. Neuropsychologia. 2002; 40:1129–1138. [PubMed: 11931917]

Caspers S, Eickhoff SB, Geyer S, Scheperjans F, Mohlberg H, Zilles K, Amunts K. The human inferior parietal lobule in stereotaxic space. Brain Struct Funct. 2008; 212:481–495. [PubMed: 18651173]

Caspers S, Eickhoff SB, Rick T, von Kapri A, Kuhlen T, Huang R, Shah NJ, Zilles K. Probabilistic fibre tract analysis of cytoarchitectonically defined human inferior parietal lobule areas reveals similarities to macaques. NeuroImage. 2011; 58:362–380. [PubMed: 21718787]

Caspers S, Geyer S, Schleicher A, Mohlberg H, Amunts K, Zilles K. The human inferior parietal cortex: cytoarchitectonic parcellation and interindividual variability. NeuroImage. 2006; 33:430–448. [PubMed: 16949304]

Caspers S, Zilles K, Laird AR, Eickhoff SB. ALE meta-analysis of action observation and imitation in the human brain. NeuroImage. 2010; 50:1148–1167. [PubMed: 20056149]

Chang SE, Kenney MK, Loucks TM, Poletto CJ, Ludlow CL. Common neural substrates support speech and non-speech vocal tract gestures. NeuroImage. 2009; 47:314–325. [PubMed: 19327400]

Choi HJ, Zilles K, Mohlberg H, Schleicher A, Fink GR, Armstrong E, Amunts K. Cytoarchitectonic identification and probabilistic mapping of two distinct areas within the anterior ventral bank of the human intraparietal sulcus. The Journal of comparative neurology. 2006; 495:53–69. [PubMed: 16432904]

Cieslik EC, Zilles K, Caspers S, Roski C, Kellermann TS, Jakobs O, Langner R, Laird AR, Fox PT, Eickhoff SB. Is there "one" DLPFC in cognitive action control? Evidence for heterogeneity from co-activation-based parcellation. Cerebral cortex. 2013; 23:2677–2689. [PubMed: 22918987]

Clos M, Amunts K, Laird AR, Fox PT, Eickhoff SB. Tackling the multifunctional nature of Broca's region meta-analytically: Co-activation-based parcellation of area 44. NeuroImage. 2013; 83C: 174–188.

Cohen AS, Sasaki JY, German TC. Specialized mechanisms for theory of mind: Are mental representations special because they are mental or because they are representations? Cognition. 2014; 136:49–63. [PubMed: 25490129]

Corbetta M, Patel G, Shulman GL. The reorienting system of the human brain: from environment to theory of mind. Neuron. 2008; 58:306–324. [PubMed: 18466742]

Decety J, Lamm C. The role of the right temporoparietal junction in social interaction: how low-level computational processes contribute to meta-cognition. Neuroscientist. 2007; 13:580–593. [PubMed: 17911216]

Dehaene S, Piazza M, Pinel P, Cohen L. Three parietal circuits for number processing. Cognitive neuropsychology. 2003; 20:487–506. [PubMed: 20957581]

Dohnel K, Schuwerk T, Meinhardt J, Sodian B, Hajak G, Sommer M. Functional activity of the right temporo-parietal junction and of the medial prefrontal cortex associated with true and false belief reasoning. Neuroimage. 2012; 60:1652–1661. [PubMed: 22300812]

Dosch M, Loenneker T, Bucher K, Martin E, Klaver P. Learning to appreciate others: neural development of cognitive perspective taking. Neuroimage. 2009; 50:837–846. [PubMed: 20025981]

Dosenbach NU, Visscher KM, Palmer ED, Miezin FM, Wenger KK, Kang HC, Burgund ED, Grimes AL, Schlaggar BL, Petersen SE. A core system for the implementation of task sets. Neuron. 2006; 50:799–812. [PubMed: 16731517]

Dunbar RIM. Gossip in Evolutionary Perspective. Rev Gen Psychol. 2004; 8:100–110.

Dunbar RIM, Duncan NDC, Marriott A. Human conversational behavior. Hum Nature. 1997; 8:231–246. [PubMed: 26196965]

Eickhoff SB, Bzdok D, Laird AR, Kurth F, Fox PT. Activation likelihood estimation meta-analysis revisited. NeuroImage. 2012; 59:2349–2361. [PubMed: 21963913]

Eickhoff SB, Bzdok D, Laird AR, Roski C, Caspers S, Zilles K, Fox PT. Co-activation patterns distinguish cortical modules, their connectivity and functional differentiation. NeuroImage. 2011; 57:938–949. [PubMed: 21609770]

Eickhoff SB, Laird AR, Fox PT, Bzdok D, Hensel L. Functional Segregation of the Human Dorsomedial Prefrontal Cortex. Cerebral cortex. 2016; 26:304–321. [PubMed: 25331597]

Eickhoff SB, Laird AR, Grefkes C, Wang LE, Zilles K, Fox PT. Coordinate-Based Activation Likelihood Estimation Meta-Analysis of Neuroimaging Data: A Random-Effects Approach Based on Empirical Estimates of Spatial Uncertainty. Hum Brain Mapp. 2009; 30:2907–2926. [PubMed: 19172646]

Eickhoff SB, Paus T, Caspers S, Grosbras MH, Evans AC, Zilles K, Amunts K. Assignment of functional activations to probabilistic cytoarchitectonic areas revisited. NeuroImage. 2007; 36:511–521. [PubMed: 17499520]

Eickhoff SB, Stephan KE, Mohlberg H, Grefkes C, Fink GR, Amunts K, Zilles K. A new SPM toolbox for combining probabilistic cytoarchitectonic maps and functional imaging data. NeuroImage. 2005; 25:1325–1335. [PubMed: 15850749]

Eickhoff SB, Thirion B, Varoquaux G, Bzdok D. Connectivity-based parcellation: Critique and implications. Human brain mapping. 2015

Engemann DA, Bzdok D, Eickhoff SB, Vogeley K, Schilbach L. Games people play-toward an enactive view of cooperation in social neuroscience. Frontiers in human neuroscience. 2012; 6:148. [PubMed: 22675293]

Fiori V, Coccia M, Marinelli CV, Vecchi V, Bonifazi S, Ceravolo MG, Provinciali L, Tomaiuolo F, Marangolo P. Transcranial direct current stimulation improves word retrieval in healthy and nonfluent aphasic subjects. J Cogn Neurosci. 2011; 23:2309–2323. [PubMed: 20946060]

Fletcher PC, Happe F, Frith U, Baker SC, Dolan RJ, Frackowiak RS, Frith CD. Other minds in the brain: a functional imaging study of "theory of mind" in story comprehension. Cognition. 1995; 57:109–128. [PubMed: 8556839]

Forgy EW. Cluster analysis of multivariate data: efficiency versus interpretability of classifications. Biometrics. 1965; 21:768–769.

Fox DF, Raichle ME. Spontaneous fluctuations in brain activity observed with functional magnetic resonance imaging. Nature reviews Neuroscience. 2007; 8:700–711. [PubMed: 17704812]

Fox MD, Zhang D, Snyder AZ, Raichle ME. The global signal and observed anticorrelated resting state brain networks. Journal of neurophysiology. 2009; 101:3270–3283. [PubMed: 19339462]

Fox PT, Laird AR, Fox SP, Fox PM, Uecker AM, Crank M, Koenig SF, Lancaster JL. BrainMap taxonomy of experimental design: Description and evaluation. Human brain mapping. 2005; 25:185–198. [PubMed: 15846810]

Fox PT, Lancaster JL. Opinion: Mapping context and content: the BrainMap model. Nature reviews Neuroscience. 2002; 3:319–321. [PubMed: 11967563]

Frith U, Frith CD. Development and neurophysiology of mentalizing. Philosophical transactions of the Royal Society of London Series B, Biological sciences. 2003; 358:459–473. [PubMed: 12689373]

Geschwind, N. Science. Citeseer: 1970. The organization of language and the brain.

Hart J Jr, Gordon B. Delineation of single-word semantic comprehension deficits in aphasia, with anatomical correlation. Annals of Neurology. 1990; 27:226–231. [PubMed: 2327733]

Hartigan JA, Wong MA. A k-means clustering algorithm. Appl Stat. 1979; 28:100–108.

Hartwigsen G, Golombek T, Obleser J. Repetitive transcranial magnetic stimulation over left angular gyrus modulates the predictability gain in degraded speech comprehension. Cortex; a journal devoted to the study of the nervous system and behavior. 2014

Heyes CM, Frith CD. The cultural evolution of mind reading. Science. 2014; 344:1243091. [PubMed: 24948740]

Hickok G, Buchsbaum BR, Humphries C, Muftuler T. Auditory–motor interaction revealed by fMRI: speech, music, and working memory in area Spt. Cognitive Neuroscience, Journal of. 2003; 15:673–682.

Hickok G, Poeppel D. Dorsal and ventral streams: a framework for understanding aspects of the functional anatomy of language. Cognition. 2004; 92:67–99. [PubMed: 15037127]

Hickok G, Poeppel D. The cortical organization of speech processing. Nature Reviews Neuroscience. 2007; 8:393–402. [PubMed: 17431404]

Holmes CJ, Hoge R, Collins L, Woods R, Toga AW, Evans AC. Enhancement of MR images using registration for signal averaging. Journal of computer assisted tomography. 1998; 22:324–333. [PubMed: 9530404]

Jain AK. Data clustering: 50 years beyond K-means. Pattern Recognition Letters. 2010; 31:651–666.

Jain AK, Murty MN, Flynn PJ. Data clustering: a review. ACN Computing Surveys. 1999; 31:264–323.

Jakobs O, Langner R, Caspers S, Roski C, Cieslik EC, Zilles K, Laird AR, Fox PT, Eickhoff SB. Across-study and within-subject functional connectivity of a right temporo-parietal junction subregion involved in stimulus-context integration. NeuroImage. 2012; 60:2389–2398. [PubMed: 22387170]

Jefferies E, Lambon Ralph MA. Semantic impairment in stroke aphasia versus semantic dementia: a case-series comparison. Brain. 2006; 129:2132–2147. [PubMed: 16815878]

Johansen-Berg H, Behrens TE, Robson MD, Drobnjak I, Rushworth MF, Brady JM, Smith SM, Higham DJ, Matthews PM. Changes in connectivity profiles define functionally distinct regions in human medial frontal cortex. Proceedings of the National Academy of Sciences of the United States of America. 2004; 101:13335–13340. [PubMed: 15340158]

Kahnt T, Chang LJ, Park SQ, Heinzle J, Haynes JD. Connectivity-based parcellation of the human orbitofrontal cortex. The Journal of neuroscience : the official journal of the Society for Neuroscience. 2012; 32:6240–6250. [PubMed: 22553030]

Kobayashi C, Glover GH, Temple E. Cultural and linguistic influence on neural bases of 'Theory of Mind': an fMRI study with Japanese bilinguals. Brain and language. 2006; 98:210–220. [PubMed: 16753205]

Kobayashi C, Glover GH, Temple E. Children's and adults' neural bases of verbal and nonverbal 'theory of mind'. Neuropsychologia. 2007; 45:1522–1532. [PubMed: 17208260]

Konishi M, McLaren DG, Engen H, Smallwood J. Shaped by the past: the default mode network supports cognition that is independent of immediate perceptual input. PloS one. 2015; 10:e0132209. [PubMed: 26125559]

Koster-Hale J, Saxe R, Dungan J, Young LL. Decoding moral judgments from neural representations of intentions. Proceedings of the National Academy of Sciences of the United States of America. 2013; 110:5648–5653. [PubMed: 23479657]

Kovacs AM, Teglas E, Endress AD. The social sense: susceptibility to others' beliefs in human infants and adults. Science. 2010; 330:1830–1834. [PubMed: 21205671]

Laird AR, Eickhoff SB, Fox PM, Uecker AM, Ray KL, Saenz JJ Jr, McKay DR, Bzdok D, Laird RW, Robinson JL, Turner JA, Turkeltaub PE, Lancaster JL, Fox PT. The BrainMap Strategy for Standardization, Sharing, and Meta-Analysis of Neuroimaging Data. BMC Res Notes. 2011; 4:349. [PubMed: 21906305]

Laird AR, Eickhoff SB, Kurth F, Fox PM, Uecker AM, Turner JA, Robinson JL, Lancaster JL, Fox PT. ALE Meta-Analysis Workflows Via the Brainmap Database: Progress Towards A Probabilistic Functional Brain Atlas. Front Neuroinformatics. 2009; 3:23.

Laird AR, Eickhoff SB, Rottschy C, Bzdok D, Ray KL, Fox PT. Networks of task coactivations. NeuroImage. 2013; 80:505–514. [PubMed: 23631994]

Lambon Ralph MA, Patterson K. Generalization and differentiation in semantic memory: insights from semantic dementia. Ann N Y Acad Sci. 2008; 1124:61–76. [PubMed: 18400924]

Li JM, Bentley WJ, Snyder AZ, Raichle ME, Snyder LH. Functional connectivity arises from a slow rhythmic mechanism. Proceedings of the National Academy of Sciences. 2015; 112:E2527–E2535.

Lien MC, Allen P, Martin N. Processing visual words with numbers: electrophysiological evidence for semantic activation. Psychon Bull Rev. 2014; 21:1056–1066. [PubMed: 24436053]

Mar RA. The neural bases of social cognition and story comprehension. Annu Rev Psychol. 2011; 62:103–134. [PubMed: 21126178]

Mars RB, Jbabdi S, Sallet J, O'Reilly JX, Croxson PL, Olivier E, Noonan MP, Bergmann C, Mitchell AS, Baxter MG, Behrens TE, Johansen-Berg H, Tomassini V, Miller KL, Rushworth MF. Diffusion-weighted imaging tractography-based parcellation of the human parietal cortex and comparison with human and macaque resting-state functional connectivity. The Journal of neuroscience : the official journal of the Society for Neuroscience. 2011; 31:4087–4100. [PubMed: 21411650]

Mars RB, Sallet J, Neubert FX, Rushworth MF. Connectivity profiles reveal the relationship between brain areas for social cognition in human and monkey temporoparietal cortex. Proc Natl Acad Sci U S A. 2013; 110:10806–10811. [PubMed: 23754406]

Mars RB, Sallet J, Schuffelgen U, Jbabdi S, Toni I, Rushworth MF. Connectivity-Based Subdivisions of the Human Right "Temporoparietal Junction Area": Evidence for Different Areas Participating in Different Cortical Networks. Cerebral cortex. 2012; 22:1894–1903. [PubMed: 21955921]

Meinzer M, Jahnigen S, Copland DA, Darkow R, Grittner U, Avirame K, Rodriguez AD, Lindenberg R, Floel A. Transcranial direct current stimulation over multiple days improves learning and maintenance of a novel vocabulary. Cortex. 2014; 50:137–147. [PubMed: 23988131]

Mesoudi A, Whiten A, Dunbar R. A bias for social information in human cultural transmission. British Journal of Psychology. 2006; 97:405–423. [PubMed: 16848951]

Mesulam MM. From sensation to cognition. Brain : a journal of neurology. 1998; 121(Pt 6):1013–1052. [PubMed: 9648540]

Muller VI, Cieslik EC, Kellermann TS, Eickhoff SB. Crossmodal emotional integration in major depression. Social cognitive and affective neuroscience. 2013

Nelson SM, Cohen AL, Power JD, Wig GS, Miezin FM, Wheeler ME, Velanova K, Donaldson DI, Phillips JS, Schlaggar BL, Petersen SE. A parcellation scheme for human left lateral parietal cortex. Neuron. 2010; 67:156–170. [PubMed: 20624599]

Newhart M, Trupe LA, Gomez Y, Cloutman L, Molitoris JJ, Davis C, Leigh R, Gottesman RF, Race D, Hillis AE. Asyntactic comprehension, working memory, and acute ischemia in Broca's area versus angular gyrus. Cortex. 2011; 48:1288–1297. [PubMed: 22079684]

Nichols T, Brett M, Andersson J, Wager T, Poline JB. Valid conjunction inference with the minimum statistic. NeuroImage. 2005; 25:653–660. [PubMed: 15808966]

Onishi KH, Baillargeon R. Do 15-month-old infants understand false beliefs? Science. 2005; 308:255–258. [PubMed: 15821091]

Orban GA, Van Essen D, Vanduffel W. Comparative mapping of higher visual areas in monkeys and humans. Trends Cogn Sci. 2004; 8:315–324. [PubMed: 15242691]

Ossmy O, Ben-Shachar M, Mukamel R. Decoding letter position in word reading. Cortex; a journal devoted to the study of the nervous system and behavior. 2014; 59:74–83. [PubMed: 25133927]

Passingham RE, Stephan KE, Kotter R. The anatomical basis of functional localization in the cortex. Nature reviews Neuroscience. 2002; 3:606–616. [PubMed: 12154362]

Poldrack RA. Can cognitive processes be inferred from neuroimaging data? Trends in cognitive sciences. 2006; 10:59–63. [PubMed: 16406760]

Price CJ. The anatomy of language: contributions from functional neuroimaging. Journal of anatomy. 2000; 197(Pt 3):335–359. [PubMed: 11117622]

Price CJ. The anatomy of language: a review of 100 fMRI studies published in 2009. Ann Ny Acad Sci. 2010; 1191:62–88. [PubMed: 20392276]

Raichle ME, MacLeod AM, Snyder AZ, Powers WJ, Gusnard DA, Shulman GL. A default mode of brain function. Proceedings of the National Academy of Sciences of the United States of America. 2001; 98:676–682. [PubMed: 11209064]

Reetz K, Dogan I, Rolfs A, Binkofski F, Schulz JB, Laird AR, Fox PT, Eickhoff SB. Investigating function and connectivity of morphometric findings - Exemplified on cerebellar atrophy in spinocerebellar ataxia 17 (SCA17). NeuroImage. 2012; 62:1354–1366. [PubMed: 22659444]

Rilling JK, Sanfey AG, Aronson JA, Nystrom LE, Cohen JD. The neural correlates of theory of mind within interpersonal interactions. NeuroImage. 2004; 22:1694–1703. [PubMed: 15275925]

Robinson JL, Laird AR, Glahn DC, Lovallo WR, Fox PT. Metaanalytic connectivity modeling: delineating the functional connectivity of the human amygdala. Human brain mapping. 2010; 31:173–184. [PubMed: 19603407]

Sabbagh MA, Xu F, Carlson SM, Moses LJ, Lee K. The development of executive functioning and theory of mind. A comparison of Chinese and U.S. preschoolers. Psychol Sci. 2006; 17:74–81. [PubMed: 16371147]

Saxe R, Kanwisher N. People thinking about thinking people. The role of the temporoparietal junction in "theory of mind". NeuroImage. 2003; 19:1835–1842. [PubMed: 12948738]

Schaafsma SM, Pfaff DW, Spunt RP, Adolphs R. Deconstructing and reconstructing theory of mind. Trends in cognitive sciences. 2015; 19:65–72. [PubMed: 25496670]

Schacter DL, Addis DR, Buckner RL. Remembering the past to imagine the future: the prospective brain. Nature reviews Neuroscience. 2007; 8:657–661. [PubMed: 17700624]

Scheperjans F, Eickhoff SB, Homke L, Mohlberg H, Hermann K, Amunts K, Zilles K. Probabilistic maps, morphometry, and variability of cytoarchitectonic areas in the human superior parietal cortex. Cerebral cortex. 2008; 18:2141–2157. [PubMed: 18245042]

Schurz M, Radua J, Aichhorn M, Richlan F, Perner J. Fractionating theory of mind: a metaanalysis of functional brain imaging studies. Neuroscience and biobehavioral reviews. 2014; 42:9–34. [PubMed: 24486722]

Seeley WW, Menon V, Schatzberg AF, Keller J, Glover GH, Kenna H, Reiss AL, Greicius MD. Dissociable intrinsic connectivity networks for salience processing and executive control. The Journal of neuroscience : the official journal of the Society for Neuroscience. 2007; 27:2349–2356. [PubMed: 17329432]

Seghier ML. The Angular Gyrus: Multiple Functions and Multiple Subdivisions. Neuroscientist. 2013:43–61. [PubMed: 22547530]

Sliwinska MW, James A, Devlin JT. Inferior Parietal Lobule Contributions to Visual Word Recognition. J Cogn Neurosci. 2014:1–12. [PubMed: 24047384]

Smith EE, Jonides J, Marshuetz C, Koeppe RA. Components of verbal working memory: evidence from neuroimaging. Proc Natl Acad Sci U S A. 1998; 95:876–882. [PubMed: 9448254]

Spreng RN, Mar RA, Kim AS. The common neural basis of autobiographical memory, prospection, navigation, theory of mind, and the default mode: a quantitative meta-analysis. Journal of cognitive neuroscience. 2009; 21:489–510. [PubMed: 18510452]

Straube B, Green A, Jansen A, Chatterjee A, Kircher T. Social cues, mentalizing and the neural processing of speech accompanied by gestures. Neuropsychologia. 2010; 48:382–393. [PubMed: 19782696]

Surian L, Caldi S, Sperber D. Attribution of beliefs by 13-month-old infants. Psychol Sci. 2007; 18:580–586. [PubMed: 17614865]

Thirion B, Varoquaux G, Dohmatob E, Poline JB. Which fMRI clustering gives good brain parcellations? Frontiers in neuroscience. 2014; 8:167. [PubMed: 25071425]

Tomasello, M. The cultural origins of cognition. Cambridge, MA: Harvard University Press; 1999.

Tomasello M, Carpenter M, Call J, Behne T, Moll H. Understanding and sharing intentions: the origins of cultural cognition. Behav Brain Sci. 2005; 28:675–691. discussion 691–735. [PubMed: 16262930]

Turkeltaub PE, Eden GF, Jones KM, Zeffiro TA. Meta-analysis of the functional neuroanatomy of single-word reading: Method and validation. NeuroImage. 2002; 16:765–780. [PubMed: 12169260]

Turkeltaub PE, Eickhoff SB, Laird AR, Fox M, Wiener M, Fox P. Minimizing within-experiment and within-group effects in Activation Likelihood Estimation meta-analyses. Human brain mapping. 2012; 33:1–13. [PubMed: 21305667]

Uddin LQ, Supekar K, Amin H, Rykhlevskaia E, Nguyen DA, Greicius MD, Menon V. Dissociable connectivity within human angular gyrus and intraparietal sulcus: evidence from functional and structural connectivity. Cerebral Cortex. 2011; 20:2636–2646.

Van Overwalle F. Social cognition and the brain: a meta-analysis. Hum Brain Mapp. 2009; 30:829–858. [PubMed: 18381770]

Varoquaux G, Thirion B. How machine learning is shaping cognitive neuroimaging. GigaScience. 2014; 3:28. [PubMed: 25405022]

Vigneau M, Beaucousin V, Herve PY, Duffau H, Crivello F, Houde O, Mazoyer B, Tzourio-Mazoyer N. Meta-analyzing left hemisphere language areas: phonology, semantics, and sentence processing. NeuroImage. 2006; 30:1414–1432. [PubMed: 16413796]

Vogeley K, May M, Ritzl A, Falkai P, Zilles K, Fink GR. Neural correlates of first-person perspective as one constituent of human self-consciousness. J Cogn Neurosci. 2004; 16:817–827. [PubMed: 15200709]

Vollm BA, Taylor AN, Richardson P, Corcoran R, Stirling J, McKie S, Deakin JF, Elliott R. Neuronal correlates of theory of mind and empathy: a functional magnetic resonance imaging study in a nonverbal task. Neuroimage. 2006; 29:90–98. [PubMed: 16122944]

Watson AC, Nixon CL, Wilson A, Capage L. Social interaction skills and theory of mind in young children. Dev Psychol. 1999; 35:386–391. [PubMed: 10082009]

Weissenbacher A, Kasess C, Gerstl F, Lanzenberger R, Moser E, Windischberger C. Correlations and anticorrelations in resting-state functional connectivity MRI: a quantitative comparison of preprocessing strategies. NeuroImage. 2009; 47:1408–1416. [PubMed: 19442749]

Weissman DH, Roberts KC, Visscher KM, Woldorff MG. The neural bases of momentary lapses in attention. Nature neuroscience. 2006; 9:971–978. [PubMed: 16767087]

Whitney C, Kirk M, O'Sullivan J, Lambon Ralph MA, Jefferies E. Executive semantic processing is underpinned by a large-scale neural network: revealing the contribution of left prefrontal, posterior temporal, and parietal cortex to controlled retrieval and selection using TMS. J Cogn Neurosci. 2012; 24:133–147. [PubMed: 21861680]

Yarkoni T, Poldrack RA, Nichols TE, Van Essen DC, Wager TD. Large-scale automated synthesis of human functional neuroimaging data. Nat Methods. 2011; 8:665–670. [PubMed: 21706013]

Yeo BT, Krienen FM, Sepulcre J, Sabuncu MR, Lashkari D, Hollinshead M, Roffman JL, Smoller JW, Zollei L, Polimeni JR, Fischl B, Liu H, Buckner RL. The organization of the human cerebral cortex estimated by intrinsic functional connectivity. Journal of neurophysiology. 2011; 106:1125–1165. [PubMed: 21653723]

Zago L, Petit L, Turbelin MR, Andersson F, Vigneau M, Tzourio-Mazoyer N. How verbal and spatial manipulation networks contribute to calculation: an fMRI study. Neuropsychologia. 2008; 46:2403–2414. [PubMed: 18406434]

Zilles K, Amunts K. Centenary of Brodmann's map--conception and fate. Nature reviews Neuroscience. 2010; 11:139–145. [PubMed: 20046193]

Highlights

- Theory of mind and language related processing facets are unlikely to be clearly dissociable in the LPL

- Cluster 1 and 2 in the ventral LPL were both congruently associated with social-cognitive and language tasks, yet in distinct functional modules

- Cluster 3 and cluster 4 in the dorsal LPL showed neither connectional nor functional evidence for a domain-specific involvement in either social or language cognitive processes
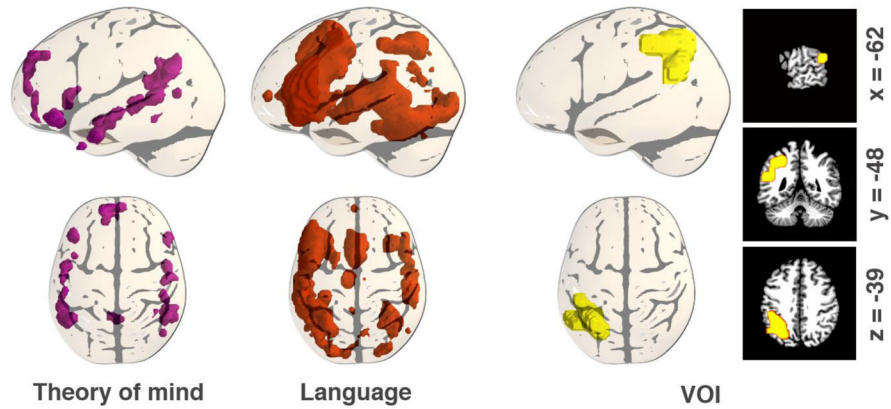
Figure 1. VOI definition

The functional volume of interest (VOI) was intended to capture consistent left parietal lobe (LPL) activation underlying social-cognitive and language tasks. One coordinate-based meta-analysis (left column) previously issued a significant activation clusters related to theory of mind (Bzdok et al., 2012). A second coordinate-based meta-analysis (middle column) on all language-associated neuroimaging experiments (i.e., orthography, speech, syntax, semantics, and phonology) hosted in the BrainMap database issued another significant activation cluster in the LPL. The social-cognition and language related activation clusters were merged to a single composite VOI (right column). This constituted the basis for all subsequent analyses.
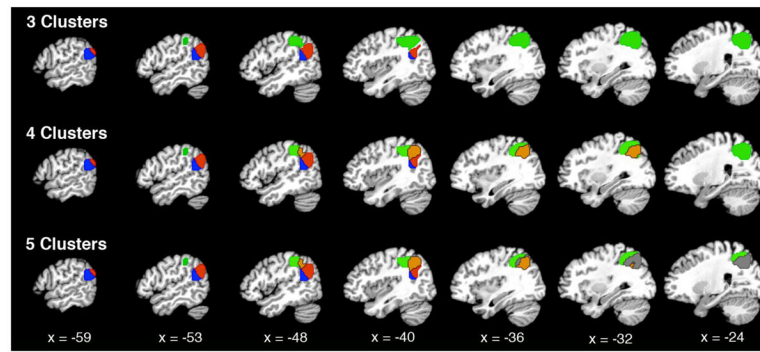
Figure 2. Anatomy of different cluster solutions

Sagittal slices of the 3 (upper row), 4 (middle row), and 5 (bottom row) cluster solutions from connectivity-based parcellation of the VOI in the left parietal lobe (Figure 1). Coordinates in MNI space.
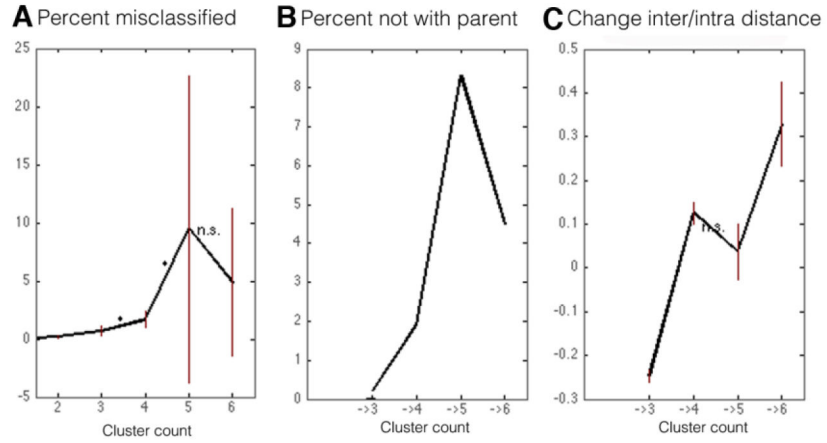
A Percent misclassified **B** Percent not with parent **C** Change inter/intra distance

Figure 3. Different clustering criteria for model selection

Three different estimates of model fit advocated the superiority of the four-cluster solution. (A) The percentage of misclassified voxels across filter sizes, (B) the percentage of voxels that lost their parent cluster with increasing clustering number showed sudden increase for solutions with more than four clusters, and (C) the change in the ratio of inter- versus intra-cluster distance accelerated from three to four cluster, yet dropped afterwards. Diverging criteria hence converged to the four-cluster solution as the best fitting model given the data. Asterisks indicate statistically significant differences and the bars indicate the standard deviation across filter sizes.
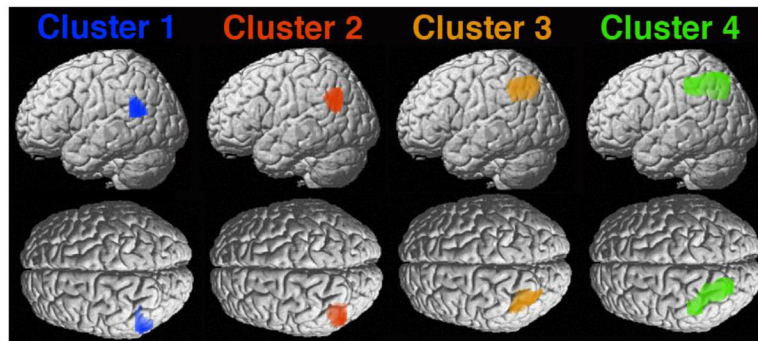
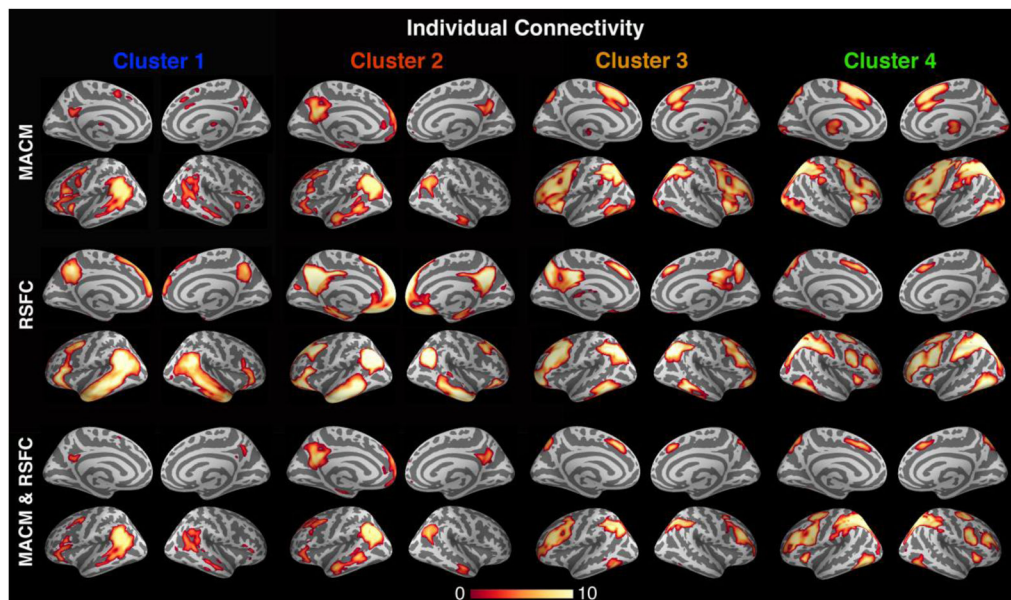**Figure 4. Rendering of the four cluster solution**

Figure 5. Individual connectivity

Individual functional connectivity patterns of the subregions of the four-cluster solution as determined using meta-analytic connectivity modeling (MACM; top two rows), resting-state connectivity (RSFC; middle two rows), and the conjunction of both methods (MACM & RSFC; bottom two rows). The significant results are rendered on left/right lateral and medial views of brain regions. Functional connectivity patterns of each cluster in the parietal VOI as individually determined using meta-analytic connectivity modeling (MACM). All results survived a cluster-corrected threshold of $p < 0.05$, corrected for multiple comparisons. The color bar on the bottom indicates z-values.
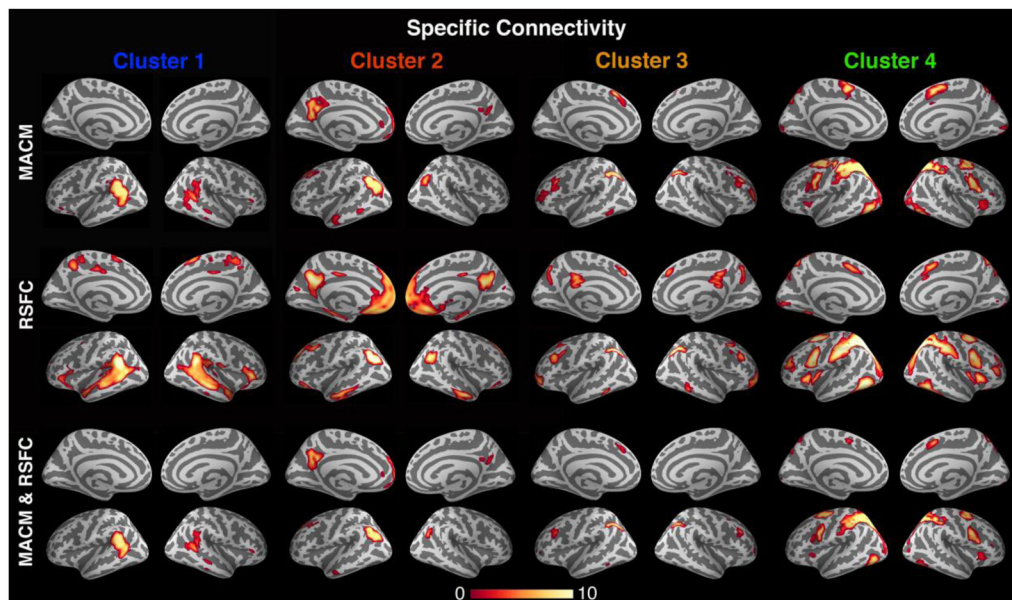
Figure 6. Specific connectivity

Specific functional connectivity patterns of the subregions of the four-cluster solution as determined using meta-analytic connectivity modeling (MACM; top two rows), resting-state connectivity (RSFC; middle two rows), and the conjunction of both methods (MACM & RSFC; bottom two rows). The significant results are rendered on left/right lateral and medial views of brain regions. Specific connectivity reflects stronger functional connectivity to a given cluster in the parietal VOI than to any of the three other clusters according to meta-analytic connectivity modeling (MACM). The color bar on the bottom indicates z-values.
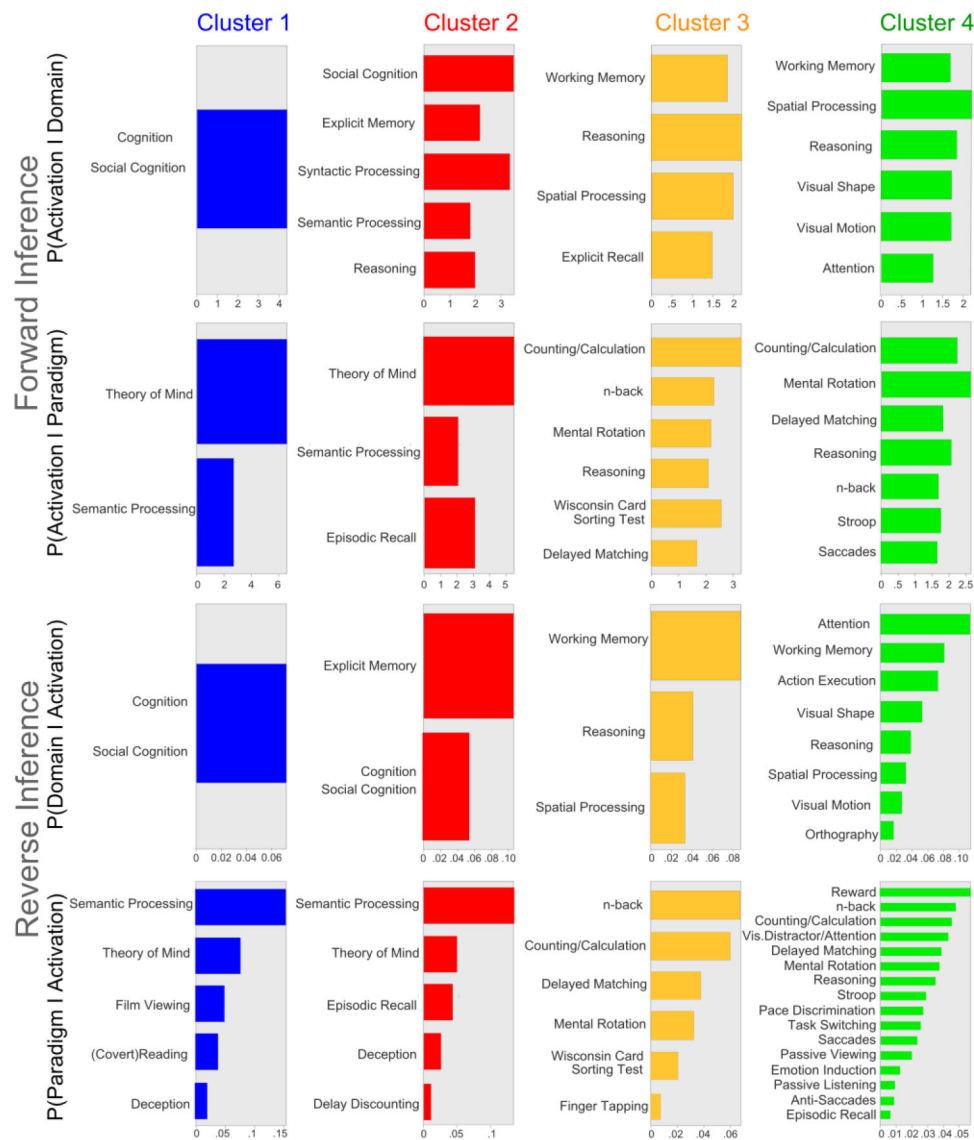
Figure 7. Functional forward and reverse decoding

Each cluster's significant association with psychological terms (Behavioral Domains and Paradigm Classes) from the BrainMap database (http://www.brainmap.org). Forward inference determines above-chance brain activity given the presence of a psychological term, whereas reverse inference determines the above-chance probability of a psychological term given the observed brain activity. All functional associations survived a significance threshold of p < 0.05. The x-axis displays relative probability values. Note that the functional decoding analysis represents a descriptive post-hoc analysis of the functional profile of *individual clusters* rather than a direct comparison *between different clusters*. The x-axis indicates relative probability values.